Ozone: Science & Engineering
The Journal of the International Ozone Association

ISSN: (Print) (Online) Journal homepage: https://www.tandfonline.com/loi/bose20

# Copper-based Layered Double Hydroxides as Heterogeneous Catalyst for Efficient Ozonation of 4-nitrophenol in Aqueous Solution: Synthesis, Characterization, and Performance Evaluation

**Abderrahmane Hiri, Ghania Radji, Rania Amiri, Achour Dakhouche & Kamel Noufel**

**To cite this article:** Abderrahmane Hiri, Ghania Radji, Rania Amiri, Achour Dakhouche & Kamel Noufel (30 Oct 2023): Copper-based Layered Double Hydroxides as Heterogeneous Catalyst for Efficient Ozonation of 4-nitrophenol in Aqueous Solution: Synthesis, Characterization, and Performance Evaluation, Ozone: Science & Engineering, DOI: 10.1080/01919512.2023.2274326

**To link to this article:** https://doi.org/10.1080/01919512.2023.2274326

Published online: 30 Oct 2023.

OZONE: SCIENCE & ENGINEERING
https://doi.org/10.1080/01919512.2023.2274326

Taylor & Francis
Taylor & Francis Group



# Copper-based Layered Double Hydroxides as Heterogeneous Catalyst for Efficient Ozonation of 4-nitrophenol in Aqueous Solution: Synthesis, Characterization, and Performance Evaluation

Abderrahmane Hiri[a], Ghania Radji[b], Rania Amiri[c], Achour Dakhouche[a], and Kamel Noufel[a]

[a]Laboratory of Inorganic Materials (LMI), University of M'sila, M'sila 28000, Algeria; [b]Laboratoire des matériaux catalytiques et procédés industriels (LMCPI), Faculté des sciences et technologies, Université Ahmed Draia, Adrar 01000, Algeria; [c]Laboratoire de Recherche Catalyse et Matériaux pour l'Environnement et les Procédés LRCMEP (LR19ES08), Faculté des Sciences de Gabès/Université de Gabès, Campus Universitaire Cité Erriadh, Gabès 6072, Tunisie

**ABSTRACT**

Co-precipitation was employed to synthesize copper-based layered double hydroxides, which were subsequently utilized as heterogeneous catalysts for the ozonation of 4-nitrophenol in aqueous solutions. Various analytical techniques, including X-ray diffraction (XRD), Fourier-transform infrared spectroscopy (FTIR), scanning electron microscopy (SEM), and thermogravimetric analysis (TGA), were utilized to characterize CuAl-$CO_3$ and $CuAl_{500}$.The catalytic activity of CuAl-$CO_3$ was evaluated under different reaction conditions. Notably, at pH 11 and 25 °C, CuAl-$CO_3$ exhibited high catalytic efficiency in the ozonation of 4NP. Increasing the catalyst dose, initial pH, and temperature led to enhanced 4NP degradation. An optimal pH of 11 and a catalyst dose of 0.3 g. $L^{-1}$ resulted in the removal of 78.6% of the initial 4NP concentration. Additionally, ozonation proved to be more efficient at temperatures of 10 °C and 55 °C. The kinetics of 4NP ozonation over CuAl-$CO_3$ and CuAl500 followed a pseudo-first-order reaction. Furthermore, the study demonstrated that CuAl-$CO_3$ and $CuAl_{500}$ exhibited stability and repeatability across multiple reaction cycles, highlighting their potential for continuous catalytic applications. Overall, this research emphasizes the effectiveness of CuAl-$CO_3$ and $CuAl_{500}$ as reliable heterogeneous catalysts for the ozonation of 4NP. The results contribute valuable insights into the development of advanced oxidation processes for the treatment of wastewater containing organic contaminants.

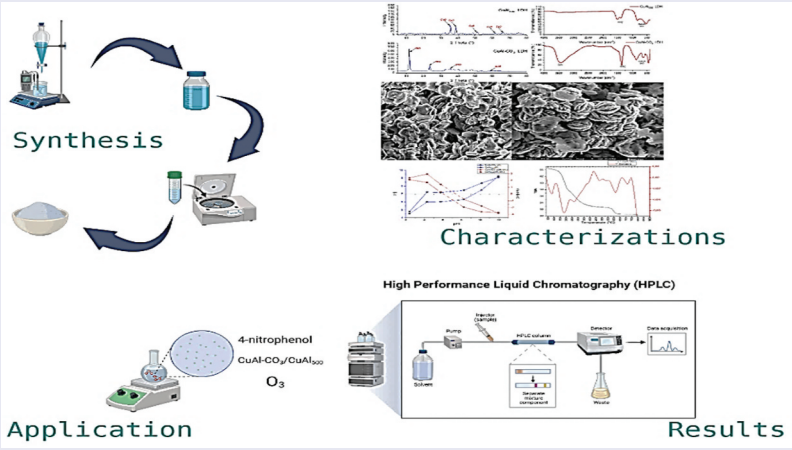


**ARTICLE HISTORY**
Received 29 August 2023
Accepted 17 October 2023

**KEYWORDS**
4-nitrophenol; Advanced oxidation process; Catalytic ozonation; Layered double hydroxides; Ozonation; Wastewater treatment

## Introduction

With uses in petrochemicals, medicines, dyes, petroleum refineries, pesticides, herbicides, and explosives, phenol and its derivatives, such as p-nitrophenol, are present in a number of productive sectors (Arasteh et al. 2010). The toxicity of 4-nitrophenol, even at low concentrations, makes it vital to emphasize the concerns associated with its presence in industrial effluents and agricultural wastes, which can contaminate nearby watercourses (Hamidouche et al. 2015). Due to the aforementioned compounds' unique properties, such as their solubility in water and the possibility for the

**CONTACT** Abderrahmane Hiri abderrahmane.hiri@univ-msila.dz Laboratory of Inorganic Materials (LMI), University of M'sila, Ichebilia, M'sila 28000, Algeria

production of substituted species, there is a risk to both human and environmental health (Kordić et al. 2018).

Nevertheless, research has shown that 4-nitrophenol is more resistant to degradation than other species of comparable size, with total destruction taking 64 days (Van, Steven and William 1980). As a result, the United States Environmental Protection Agency (USEPA) has listed 4-nitrophenol as one of the most dangerous pollutants (Mahmoud and Nabil 2017). According to the literature, the acceptable limit for 4-nitrophenol in natural waters is in the range of 0.01 and 2.0 mg/L (Kupeta, Naidoo and Ofomaja 2018). With regard to the harmful qualities of p-nitrophenol, there are already accessible water treatment strategies to eliminate this substance, including extraction (Zhang et al. 2015), photocatalytic degradation (Deng et al. 2018), electrochemical oxidation (Zaggout and Abu Ghalwa 2008), adsorption, and catalytic ozonation. This final one provides advantages such as simplicity of use, and as a result, many sorts of studies on this subject are conducted utilizing various types of catalysts, such as metal-organic frameworks (Chen et al. 2017) and modified carbon (Shao and Huang 2017).

The use of layered double hydroxides (LDH) is a new potential catalyst to remove 4-nitrophenol from fluids. Elisabetta Orfei and its collaborators studied the catalytic performance of Ni, Fe and Cu based layered double hydroxides in the removal of 4NP using $NaBH_4$ (Orfei et al. 2023). These substances are also known as hydrotalcite-like systems or anionic clays. The typical formula for these substances is $[M^{II}_{(1-x)}\ M^{III}_{x}\ (OH)_2]\ (A^{n-})_{x/n}.zH_2O$, where $M^{II}$ and $M^{III}$ are divalent and trivalent metal cations, respectively, and An-denotes an n-valent anion. As a result, these materials may be identified by the alternation of layers created by metallic divalent (like $Mg^{2+}$ or $Ni^{2+}$ or $Ca^{2+}$ or $Zn^{2+}$ or $Cu^{2+}$) and trivalent (like $Al^{3+}$ or $Fe^{3+}$) cations and interlayers containing exchangeable anions (like $CO^{2-}_3$, $NO^{2-}_3$, or $Cl^{-}$) and water molecules. Because of this, LDHs offer a wide range of synthetically feasible compositions and metal-anion combinations (Mishra, Dash and Pandey 2018). Layered double hydroxides provide great chemical stability, compositional flexibility, and a broad interlayer surface to host a variety of anionic species (Pavlovic, Ulibarri and Hermosı 2002).

An important process frequently employed to eliminate harmful chemicals from environmental media is the ozonation of p-nitrophenol. Although it has been shown that catalysts (such as metals supported on oxide powders) can speed up chemical processes (such as the reduction of nitrophenol), catalytic ozonation of 4-nitrophenol (4NP) with $CuAl\text{-}CO_3$ and $CuAl_{500}$ was investigated in this study.

## Experimental

### Reagents

The chemicals used to create $CuAl\text{-}CO_3$ and $CuAl_{500}$ were $CuCl_2.2\,H_2O$ (Sigma-Aldrich, 99%), $Al_2O_{12}\,S_3.18\,H_2O$ (Biochem, 99%), NaOH (Biochem, 97%), and $Na_2CO_3$ (Sigma-Aldrich, 99.5%). 4-nitrophenol Reagent Plus® (purity >99%) from Sigma Aldrich was used to make a standard solution of the compound. All experimental solutions were made from the stock solution by adding deionized water, Acetonitrile HPLC Plus (Sigma-Aldrich 99.9%) was used for the HPLC system, while Hydrochloric Acid ACS Reagent (MERK, 37%) and NaOH (Biochem, 97%) were employed to stabilize pH. The stock solution was used to produce all experimental solutions. All chemicals were used without any purification beforehand.

### $CuAl\text{-}CO_3$ and $CuAl_{500}$ catalyst synthesis procedure

The $CuAl\text{-}CO_3$ material containing carbonate ions intercalation was created using the co-precipitation technique illustrated in (Figure 1) in aqueous solutions at a constant pH of 10, a molar ratio of $Cu^{2+}/Al^{3+}$ of 2. A 200 mL solution with the proper concentrations of the metal ions $Cu^{2+}$ and $Al^{3+}$ was added dropwise to a basic solution of NaOH and $Na_2CO_3$, which was then constantly agitated for three hours. To facilitate the crystallization of the existing structure, the mixture had to ripen by being kept at 70 °C for 18 h. They were then collected and given several rinses in distilled water to remove the previously present sodium, chloride, and sulfate ions. The final item was cleaned and 20 h of drying at 80 °C were followed by homogeneous powder production. Some of the powder generated was subjected to a 6-h calcination process at 500 °C to create calcined $CuAl_{500}$ LDH.

### $CuAl\text{-}CO_3$ and $CuAl_{500}$ catalysts characterization

Powder X-ray diffraction (XRD) patterns were recorded using a monochromatic Cu-K1 radiation source and a PXRD Porto benchtop power diffraction equipment. They were recorded throughout an angular range of 5–80 degrees with 0.02-degree steps and a 2-second step-counting interval. An x-ray tube made of copper that was running at 30 kV and 20 mA produced cu-k radiation. The PANalytical X'pert HighScore Plus software was used to process and evaluate patterns. The phases

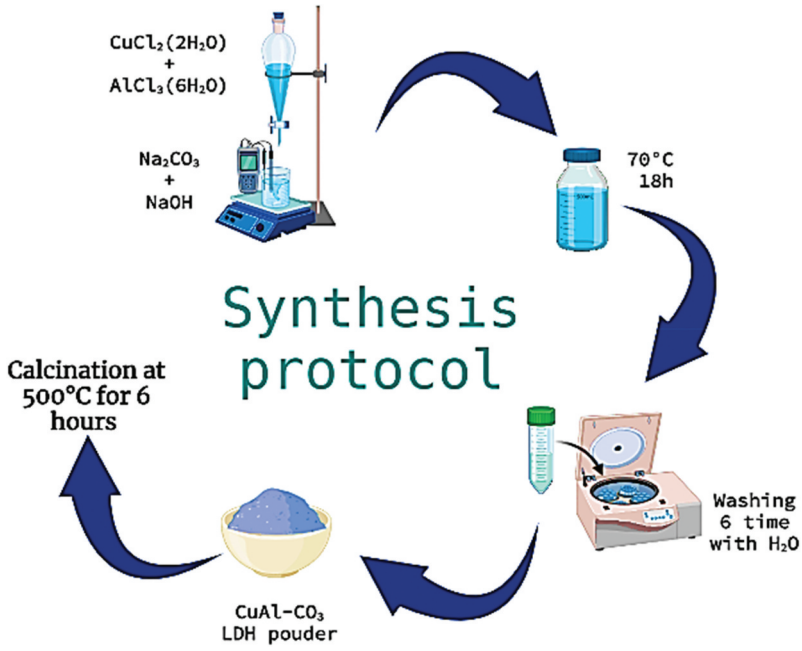


**Figure 1.** Synthesis of CuAl-$CO_3$ LDH $CuAl_{500}$ LDH protocol.

were identified using the American Mineralogist crystal structure database and the Crystallography Open Database (COD, 2019).

Catalysts are examined using an Agilent Technologies spectrophotometer. The KBr was used as a support after pelletizing, and the investigation's spectral spectrum spans from 4000 $cm^{-1}$ to 400 $cm^{-1}$.

To confirm the shape of the produced catalysts, a Quattro Environmental Scanning Electron Microscope (ESEM) for the investigation of materials in their natural form was utilized.

The BET surface areas and nitrogen adsorption-desorption of our catalysts were determined using the Brunauer- Emmet-Teller (BET) technique, using N2 physisorption analysis utilizing QuandraSorb SI Models 4.0 with the QuandraWin Software (quantachrome Instruments, v. 5.0 + newer) instrument at 77 K. Prior to measurement, each sample was outgassed for 6 h at 373 K in the instrument pre-chamber (FloVac Degasser, Quantachrome Instruments) under vacuum (6 mTorr) to eliminate adsorbed species.

Studies involving thermogravimetry were carried out using the TGA 51 Shimadzu. Samples were heated at a constant rate of 10 °C per minute to 900 °C.

The point of zero charge ($pH_{PZC}$) was determined using the salt addition technique at room temperature, according to (Radji et al. 2022):

(1) A 25 mL solution between the pHs of 2 and 12 was prepared;
(2) 1 M of either HCl or 1 M of NaOH was added to the solution to adjust the pH;
(3) 25 mg of each catalyst was added to the solution and stirred for 24 h;
(4) after decantation, the final pH of the solution was measured, and the following curves were drawn: $pH_i$ and $pH_f$ have the formulas $pH_f = f(pH_i)$ and $(pH_f\text{-}pH_i) = f(pH_i)$.

For measuring pH, an Adwa pH-meter (model AD1030) was used, and the Sigma 2-16P centrifuge (made by Hettich, Germany) was utilized for the catalyst production. The suspended elements that were most likely present in the actual samples were taken out using a Millipore membrane filter (0.45 µm).

### *Catalytic ozonation process*

Heterogenous Ozone experiments were conducted with a 100 mL solution in a glass flask. Ozone (500 mg $h^{-1}$) was introduced with magnetic stirring to CuAl-$CO_3$ and $CuAl_{500}$ catalyst. The mixture was maintained at the temperature necessary for a 30-min reaction.

The quantity of catalyst, the temperature, and the pH of the solution were just a few of the many factors that looked at as they affected the ozonation. The starting concentration of 4-Nitrophenol was adjusted at 100 mg/l, and the catalyst quantity was modified from 0.1 to 0.6 g $L^{-1}$. An oxidation with 500 mg $h^{-1}$ of $O_3$ was carried out for 30 min. Using the same method, the temperature

of the 4-Nitrophenol oxidation process was changed from 10 to 65 °C.

Indicating the quantity of the catalyst at 0.3 g $L^{-1}$ and the 4-nitrophenol concentration at 100 mg $L^{-1}$. The solution's pH ranged from 3 to 11. After the experimental conditions are optimized, the elimination of the COD in 4 h is monitored, and a kinetic analysis to ascertain the reaction's rate constant is also assessed.

Finally, we compared the two catalysts CuAl-$CO_3$ and $CuAl_{500}$ LDHs by looking at the kinetics of the reaction using the $CuAl_{500}$ catalyst in 1 h and its efficiency in reducing COD in 4 h using the phenomenon under the same previous optimum conditions (catalyst mass of 0.3 g.$L^{-1}$, concentration 100 mg. $L^{-1}$, ambient temperature, and solution pH without modification = 5.42).

The HPLC system (1220 LC System VL) was made up of the Waters quaternary pump, VWD detector, manual injector, and OpenLab software for peak detection and integration. Chromatographic separation was carried out using an Agilent Technologies C18 column that has a length of 150 mm, 5 µm, and 4.6 mm. The mobile phase was supplied at a flow rate of 1 mL.$min^{-1}$ through the separation column and was composed of a 40:60 volume ratio of water and acetonitrile. The UV detector was operated at a wavelength of 318 nm to detect 4-nitrophenol.

## Results and discussions

### *CuAl-$CO_3$ and $CuAl_{500}$ characterizations*

The evolution of the composition may be followed using thermogravimetric analysis (TGA), which demonstrates how a sample's mass changes with temperature. In general, variables like the nature of the cations, cationic compositions, the nature of the inter-lamellar anions, the crystallinity of the material, etc. affect how thermally stable LDH materials are.

By looking at the thermograms of our CuAl-$CO_3$ LDH catalysts in Figure 2, we could see the multi-step mass loss of type 4 according to the shape-based TGA curve categorization.

They demonstrated that our materials had undergone a multi-step breakdown process, as has frequently been described in the literature (Radji et al. 2022).

Following is an overview of the theories proposed to account for these losses, particularly the most significant ones:

(1) loss of physiosorbed water between 60 and 100 °C.

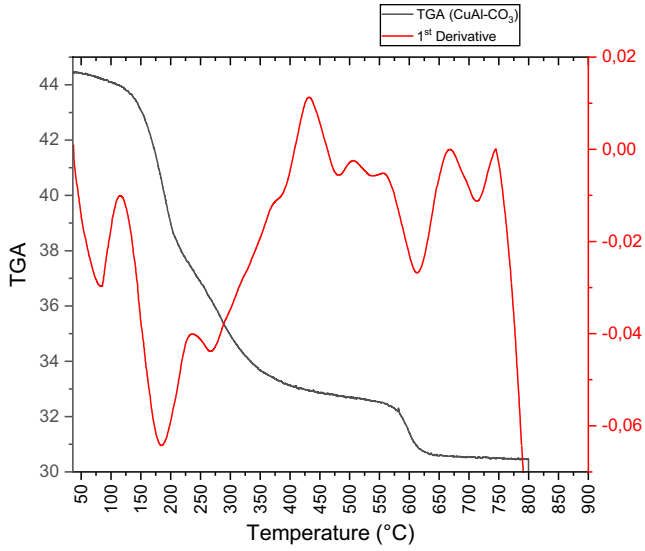


**Figure 2.** TGA analysis of CuAl-$CO_3$ LDH and its 1st derivative.

(2) departure of structural water molecules between 150 and 200 °C.

(3) departure of a substantial number of carbonates beyond 250 °C, leading to the disintegration of the lamellar phase and the creation of oxides.

Diffraction peak series at 11°, 23°, 35°, and 60° are visible in the CuAl-$CO_3$ LDH sample's XRD pattern in (Figure 3). These peaks are consistent with crystal plane reflections (003), (006), (009), and (110) in the LDH phase (Choi, Tan Lee and Bong Lee 2023). A comparison between the identification and the (Dubey, Rives and Kannan 2002) data was made. The broad diffraction peaks reveal the relatively small particle size. Scherrer's equation was employed to calculate the crystallite size in order to confirm this presumption, and the findings revealed that the average crystallite size was 1.56 nm. Additionally, the strong (003) diffraction peak is a result of the sequential stacking of layers along the c-axis (Zhang et al. 2005), as evidenced by the basal spacing d (003) (0.76 nm), which is the same as the value previously reported in the literature (Zhang et al. 2005). As a result, we can draw the conclusion that layered structures hydrotalcite-like are obtained.

According to the results of the XRD examination of the heat-treated materials, weakly crystalline copper oxide with the Hightscore COD2019 and peaks at 2Θ, 36,39 and 68 degrees was formed Figure 3. In compared to a pure copper oxide, these peaks are somewhat displaced to higher 2Θ angles. This is a result of the addition of aluminum to the CuO framework, which led to the synthesis of a mixed-metal oxide. There were no peaks identified as transition metal oxides. $CuAl_{500}$

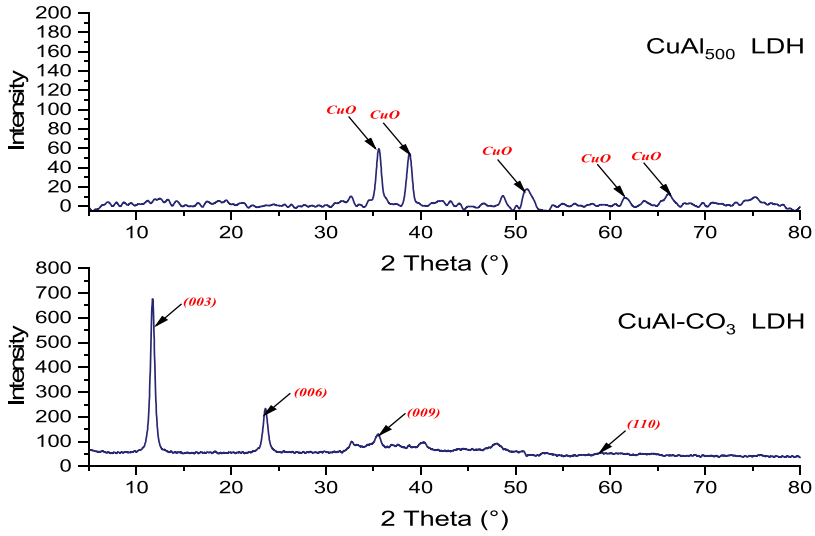


**Figure 3.** XRD diffractogram of CuAl-$CO_3$ and $CuAl_{500}$ LDH.

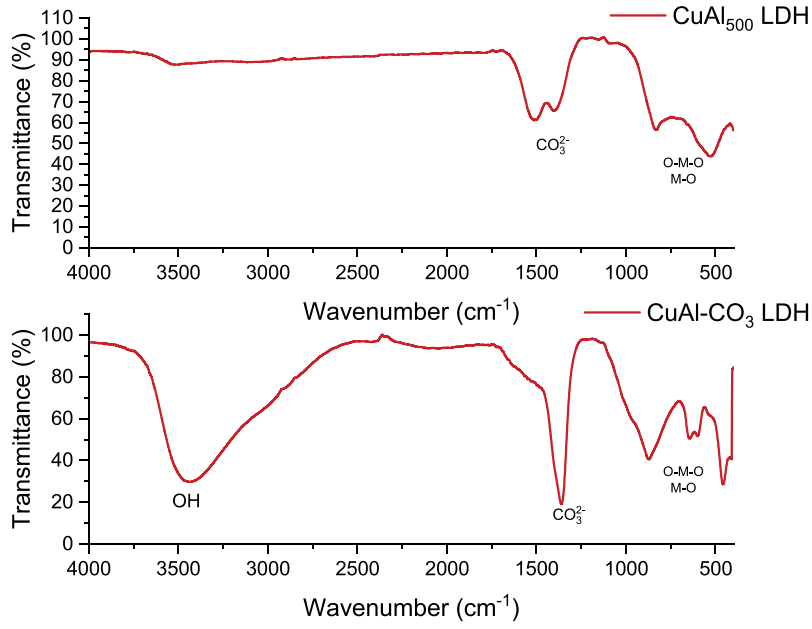


**Figure 4.** FTIR Spectrum of CuAl-$CO_3$ and $CuAl_{500}$ LDH.

LDH sample XRD patterns do not exhibit the development of spinel-type crystalline phases.

Using the FTIR approach, it is possible to recognize the LDH's internal structures as well as the intercalated anions between LDH layers. Figure 4 presents the FTIR spectra of CuAl-$CO_3$ LDH. In a wide absorption band in the vicinity of 3300–3500 $cm^{-1}$, the OH stretching frequency of the CuAl-$CO_3$ LDH was seen (Benito et al. 2008; Choi, Tan Lee and Bong Lee 2023)– (Xu and Zeng 1998). For both asymmetric and symmetric stretching vibration, the absorption bands associated with the carbonate anion generally emerged at around 1450 and 880 $cm^{-1}$, respectively (Prikhod'ko et al. 2001; Rajamathi and Kamath 2003). It was determined that the MO and OMO (M: Cu or Al) stretching vibrations were responsible for two distinct absorption bands at 590, 637 $cm^{-1}$. Due to the AlO bond associated with the $[AlO_6]^{3-}$ structure, a medium absorption band (450 $cm^{-1}$) is visible in the CuAl-$CO_3$ LDH spectrum (Choi, Tan Lee and Bong Lee 2023; Prikhod'ko et al. 2001; Radji et al. 2022; Rajamathi and Kamath 2003).

The calcinated product's infrared spectrum represented in (Figure 4) reveals a relative reduction in the strength of the absorption bands typical of water molecules (at around 3400 $cm^{-1}$ and 1640 $cm^{-1}$).

Additionally, we noticed that the band around 1359–1389 $cm^{-1}$ is still audible. While the bands recorded below 1000 $cm^{-1}$ primarily correspond to the modes produced by the spinal phase, the low intensity of this strip, compared to that observed for the starting material, suggests that carbonate ions are adsorbed to the surface of the grains of the calcinated material. The presence of these would be caused by atmospheric carbon dioxide contamination (Cavani, Trifirò and Vaccari 1991; Radji et al. 2022).

Figure 5a depicts the LDH sample's morphology. In the CuAl-$CO_3$ LDH, hexagonal plate-shaped precipitates were formed.

Polyhedral crystals were produced in the CuAl-$CO_3$ LDH. Consequently, the hexagonal plate-shaped crystals probably developed under low supersaturation environments (Taishi et al. 2015).

The CuAl- $CO_3$ LDH material is confirmed to be made of aluminum, copper, oxygen, and carbon by the EDS analysis shown in Figure 5b. The creation of the hydrotalcite-type material is attested to by these data, which also demonstrate the purity of the synthesized components and show that they underwent stringent washing procedures.

In the $CuAl_{500}$, precipitates in the shape of flowers were appeared according to Figure 6a. The irregularly shaped precipitates may be low-crystalline LDH and/or γ-AlOOH, whereas the flower-shaped precipitates were $CuAl_{500}$ crystals (Taishi et al. 2015).

In order to demonstrate the decarbonatation of the LDH and the loss of the intercalary anions, the EDS analysis of $CuAl_{500}$, shown in Figure 6b, indicates that the material is made of aluminum, copper, oxygen, and no carbon was founded. The creation of the mixed oxides substance is attested by these findings, which also demonstrate the purity of the synthesized components.

To investigate the specific surface area, the $N_2$ adsorption-desorption isotherms of the produced samples were obtained (Figure 7). The isotherm type IV was identified for CuAl-$CO_3$ LDH, and $CuAl_{500}$ LDH, indicating the mesoporous nature of the synthesized materials, according to IUPAC classification. Similarly, previous research showed CuAl-$CO_3$ LDH isotherm

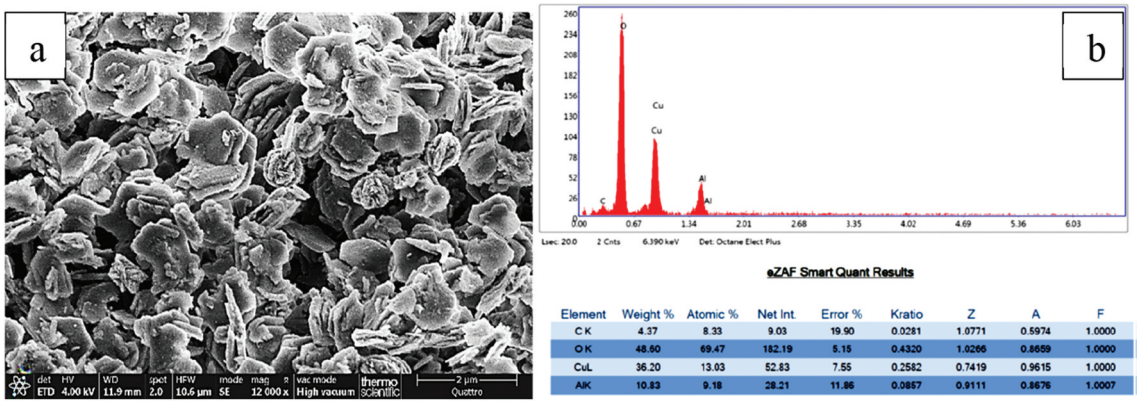


**Figure 5.** (a) SEM image of CuAl-$CO_3$ LDH (b) EDS analysis of CuAl-$CO_3$.

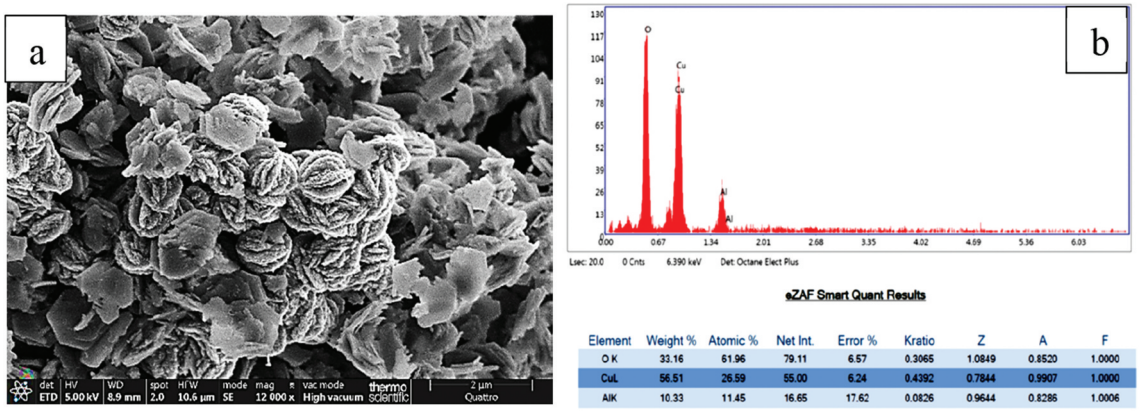


**Figure 6.** (a) SEM image of $CuAl_{500}$ LDH (b) EDS analysis of $CuAl_{500}$ LDH.

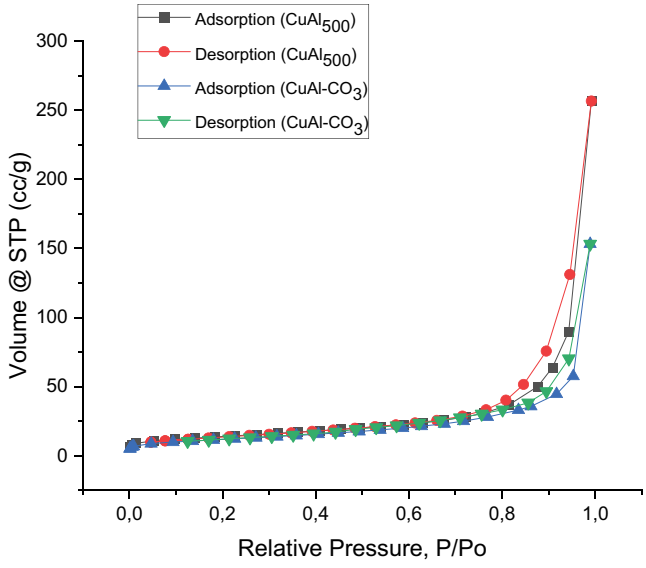


**Figure 7.** $N_2$ adsorption-desorption isotherms curves of CuAl-$CO_3$ and $CuAl_{500}$ catalysts.

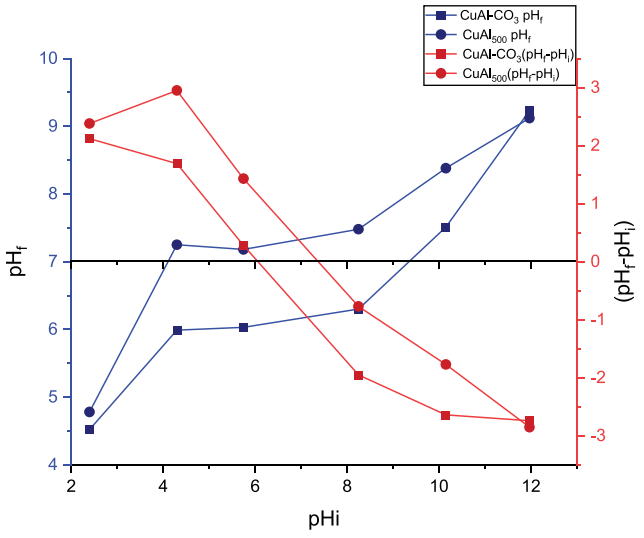


**Figure 8.** Plot of the $pH_{PZC}$ of CuAl-$CO_3$ and $CuAl_{500}$.

type IV (Radji et al. 2022). CuAl-$CO_3$ LDH had a BET surface area of 7.831 $m^2.g^{-1}$, which grew to 49.067 $m^2.g^{-1}$ after 500 °C calcination.

The CuAl-$CO_3$ and $CuAl_{500}$ LDH $pH_{PZC}$ curve is shown in Figure 8. There were identified as follows: 1) the domain in which pH < pHPZC: pHf increases with increasing pHi; the surfaces of these LDH are positively charged due to the protonation process of the hydroxyl, so our sample transforms into an anion adsorbent; 2) the domain in which pH > $pH_{PZC}$: $pH_f$ decreases with increasing $pH_i$; the surfaces of these LDH are negatively charged due to the deprotonation process of the hydroxyl, thus making our sample a cation adsorbent; The point of zero charge, or $pH_{PZC}$, is in the third domain, the intermediate domain, where $pH_f$ remains constant while $pH_i$ increases (Mak Yu et al. 2019; Radji et al. 2022). The PHpzc values of the CuAl-$CO_3$ and $CuAl_{500}$ catalysts in our case are 6.1 and 7.4, respectively.

## *Catalytic activity*

The oxidation characteristics of a solution of 4-nitrophenol (4NP) ([4NP] = 100 mg $L^{-1}$) are improved in this part using ozone as an oxidant and CuAl-$CO_3$ and $CuAl_{500}$ materials as catalysts. To evaluate the efficacy of the strategy, three pilot trials were carried out. For the first test, the material was exposed to the 4NP solution for one hour in order to determine how well the 4NP adsorbs on the catalyst. In contrast to the second test, which involved an hour-long oxidation of 4NP using just $O_3$, the third test used an hour-long catalytic oxidation of 4NP (4NP+$O_3$+catalyst). According to the results, catalytic oxidation must be done in order to drastically lower 4NP levels. We must adjust the factors that affect catalytic oxidation, such as catalyst concentration, pH, temperature, and reaction duration.

CuAl-$CO_3$ LDH in a mass series ranging from 100 to 600 mg. $L^{-1}$ was evaluated by monitoring the operation's progress for 30 min in order to find the ideal mass of CuAl-$CO_3$ LDH as a catalyst for the ozone-induced degradation of 4NP.

The mass of the catalyst increases along with an increase in conversion rate Figure 9; this rise is caused by an increase in the quantity of active sites on the catalyst's surface (Guzman-Perez, Soltan and Robertson 2011; Huang et al. 2017). A little drop appears above a mass of the catalyst corresponding to

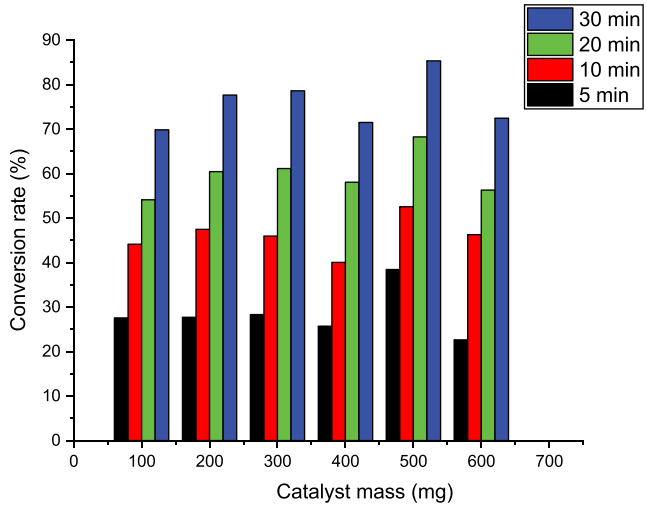


**Figure 9.** The effect of CuAl-$CO_3$ mass on the ozonation of 4NP.

300 mg. $L^{-1}$, which may be the consequence of the superposition of the active sites, which inhibits the pollutants from adhering to the surface of our catalyst. When the mass is 500 mg. $L^{-1}$, a rise is then seen, demonstrating that the number of active sites was formerly more substantial. Ozone degassing can reduce yield when the mass is 600 mg. $L^{-1}$due of the critical catalyst concentration.

The rate of ozone decomposition in aqueous solutions is greatly influenced by pH, and it accelerates as pH rises (Beltran 2003). According to Figure 10, which depicts the results of studies performed at pH values of 3.2, 6, 8.3, 10 and 11.8, the removal efficiency rose from 60 to 99% in 30 min of reaction as the pH climbed from 3.2 to 11.8, with 11.8 serving as the process' ideal pH (Shokri, Mahanpoor and Soodbar 2016). Since there were relatively few hydroxyl radicals formed at pH = 3.2, there were only limited radical reactions. At acidic conditions, the direct molecular ozonolysis was quite prevalent. Ozone was immediately reacted with the pollutant, and it appeared that the double bonds of the 4NP ring were disrupted by the ozonolysis. The potent oxidants known as hydroxyl radicals, on the other hand, are created when ozone and hydroxide ions mix at high pH. Chain oxidation of ozone began with the nonselective and quick action of hydroxyl radicals (Shokri 2016). On the other hand, beyond the pH value 6.1 (pHpzc) as was already mentioned in the pHpzc section, the surface of our catalysts is negatively charged while an attraction between the nitro function of 4NP and the surface of the catalyst is resulting therefore a better reduction efficiency is achieved (Radji et al. 2022).

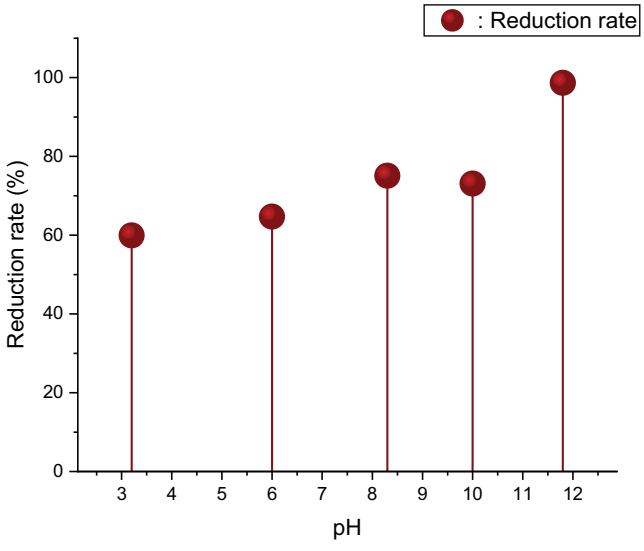


**Figure 10.** pH effect on the heterogenous ozonation of 4NP using CuAl-$CO_3$ LDH.

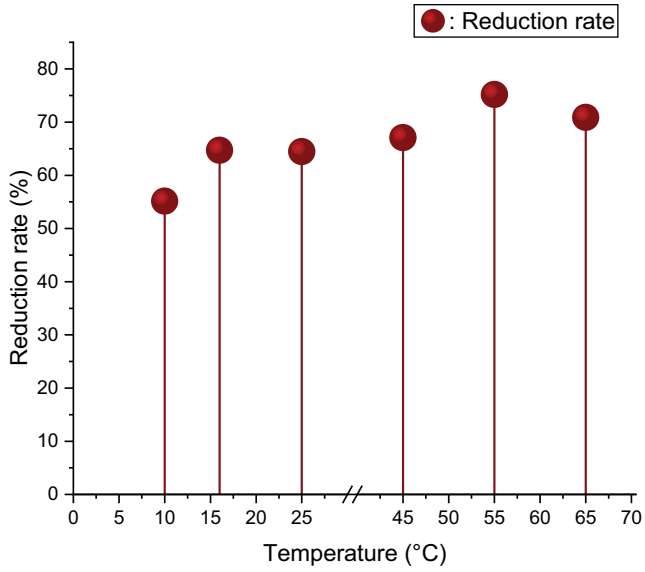


**Figure 11.** Temperature effect on the heterogenous ozonation of 4NP using CuAl-$CO_3$ LDH.

Studying how the temperature affects the catalytic ozonation of 4NP is desirable since this parameter is a kinetic component (Sumegová, Derco and Melicher 2013). Figure 11 illustrates how the temperature of the reaction solution affects the rate at which ozonation treatment reduces 4NP by altering the temperature from 15 to 70 °C.

Due to ozone's extremely high solubility in water at low temperatures (15 °C), it has been observed that ozonation is most effective at these lower temperatures. Additionally, an increase in temperature is accompanied by a noticeably faster rate of 4NP reduction. It is thus because the temperature has a kinetic effect that speeds up the reaction and increases the yield of 4NP elimination. The yield of the reaction is lowered at a very high temperature (70 °C), and this reduction may be caused by ozone's degassing and subsequent instability in the solution (Degrémont-Suez, Rueil-Malmaison, C diff Lavoisier 2005).

The results obtained demonstrate that catalytic ozonation is more effective for reducing COD, where we observe an almost complete elimination of the 4NP in less than 4 h. Figure 12 represents the evolution of the COD removal efficiency for Ozone dose effect in the catalytic ozonation of 4NP using the material CuAl-$CO_3$. Additionally, we can see that the pH of the solution is decreasing, which may be caused by the development of byproducts (acids) in the solution.

When comparing the COD reduction results of the 4NP by $CuAl_{500}$ catalytic ozonation method, as illustrated in Figure 13, it is discovered that the yield achieves a maximum of 72% in 4 h (15 g.$L^{-1}$ $O_3$).

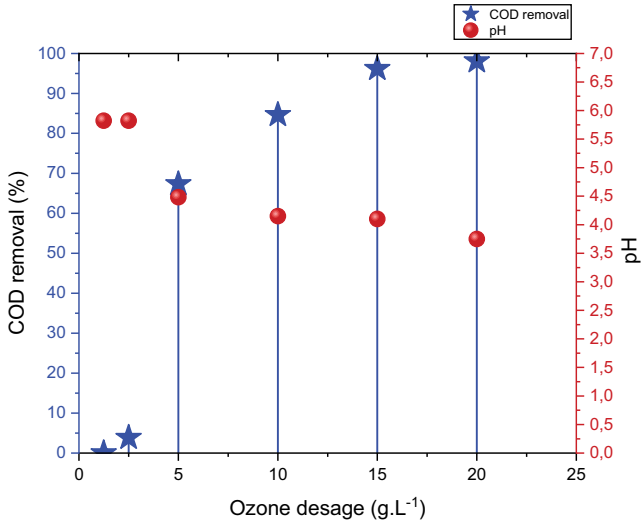


**Figure 12.** COD removal via enhanced ozonation using CuAl-$CO_3$ LDH.

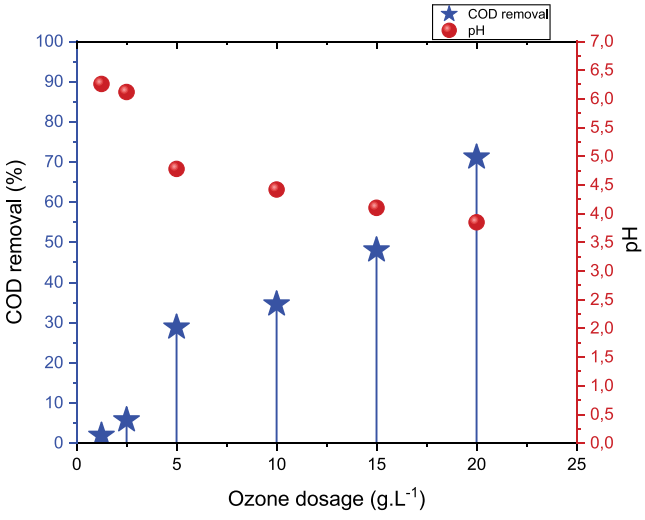


**Figure 13.** COD removal via enhanced ozonation using $CuAl_{500}$ LDH.

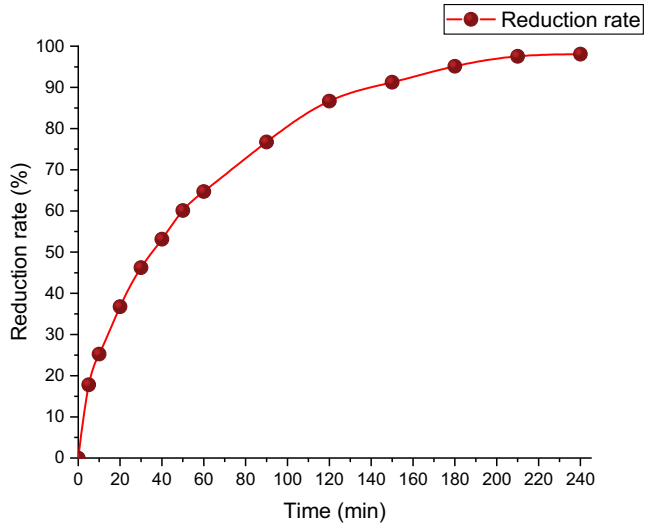


**Figure 14.** Contact time effect on the removal of 4NP by catalytic ozonation by CuAl-$CO_3$ LDH.

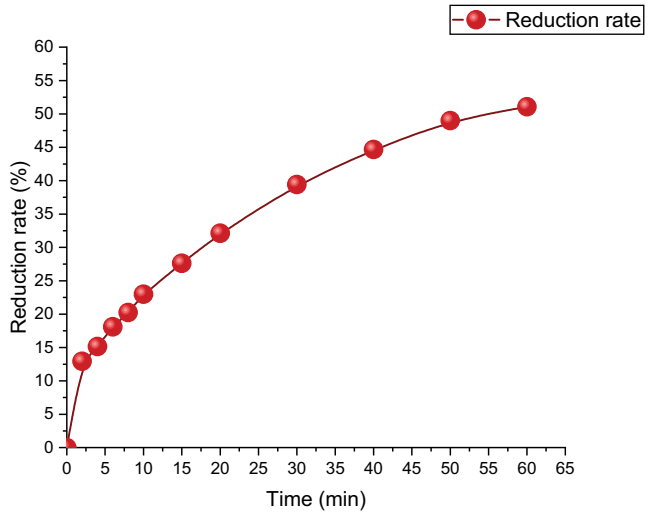


**Figure 15.** Contact time effect on the removal of 4NP by catalytic ozonation by $CuAl_{500}$ LDH.

While our catalyst's carbonated phase performs better than its calcined phase. By figuring out the rate constant, this theory will be verified.

We may understand the kinetic phenomena of our reaction by tracking the reaction through time. We display the rate% reduction as a function of time in Figure 14, and it is evident that after 4 h of catalytic ozonation (15 $g.L^{-1}$ $O_3$) with CuAl-$CO_3$, our reaction is nearly complete. The results achieved using $CuAl_{500}$ as the catalyst are shown in Figure 15, although the reaction only achieves its maximum of 51% after 1 h (5 $g.L^{-1}$ $O_3$), which is lower than the results obtained using CuAl-$CO_3$ (67%).

At the ideal pH of 5, a kinetic investigation for the degradation of 4NP in the catalytic ozonation process was carried out. The following Eq. 1 is an introduction to the kinetic relation for 4NP degradation via the indicated process:

$$\frac{-d[4NP]}{dt} = K_{O3}[4NP][Catalyst][O_3] + K_{OH^\bullet}[4NP][Catalyst][OH^\bullet]$$

Where [4NP], [$O_3$], [$OH^\bullet$] and [Catalyst] are the concentrations of 4NP, ozone, hydroxyl radicals and (CuAl-$CO_3$ or $CuAl_{500}$) LDHs, respectively. Moreover $K_{OH}$.. and $K_{O3}$ are the rate constants of

4NP with hydroxyl radicals and ozone. The kinetic equation may be expressed as follows Eq. 2, because molecular ozone and 4NP have more effective selective reactions at low pHs (Shokri 2016).

$$\frac{-\mathrm{d}[4\mathrm{NP}]}{\mathrm{dt}} = \mathrm{K}_{O3}[4\mathrm{NP}][\mathrm{Catalyst}][\mathrm{O}_3]$$

Because 4NP was eliminated in this process by reaction with (CuAl-$CO_3$ or $CuAl_{500}$) and $O_3$, and because the ratio of 4NP to $O_3$ or (CuAl-$CO_3$ or $CuAl_{500}$) was low, the concentration of $O_3$ and catalyst can be thought of as constant. Under these circumstances, the only thing that changed was the concentration of 4NP, and the reaction may be assumed to be pseudo first order (Gottschalk, Libra and Saupe 2010). Thus, the equation rate may be represented as: Equation 3:

$$\frac{-\mathrm{d}[4\mathrm{NP}]}{\mathrm{dt}} = \mathrm{K'}_{O3}[4\mathrm{NP}]$$

Where K,' is a pseudo-first order rate reaction between 4NP and an $O_3$/catalyst. Equation 3 was integrated, resulting in the equation shown below Eq. 4

$$-\ln\frac{[4\mathrm{NP}]}{[4\mathrm{NP}]_0} = \mathrm{K'}_{O3}t$$

Where [4NP] and $[4NP]_0$ represent the concentration of 4NP in the instant t and the initial concentration of 4NP respectively

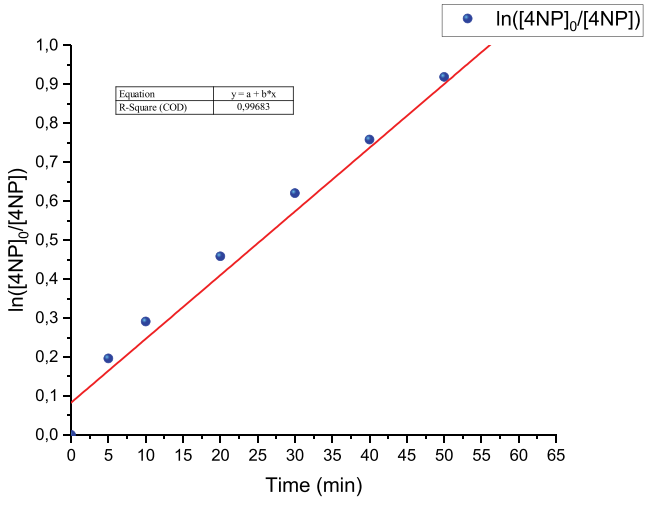


Figure 16. Kinetic modeling of the heterogenous catalytic ozonation of 4NP by CuAl-$CO_3$ LDH (K'=0,984 $min^{-1}$).

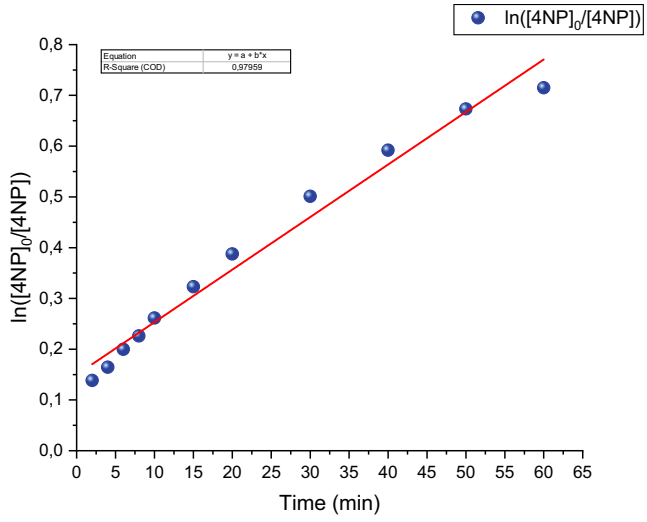


Figure 17. Kinetic modeling of the heterogenous catalytic ozonation of 4NP by $CuAl_{500}$ LDH (K'=0.624 $min^{-1}$).

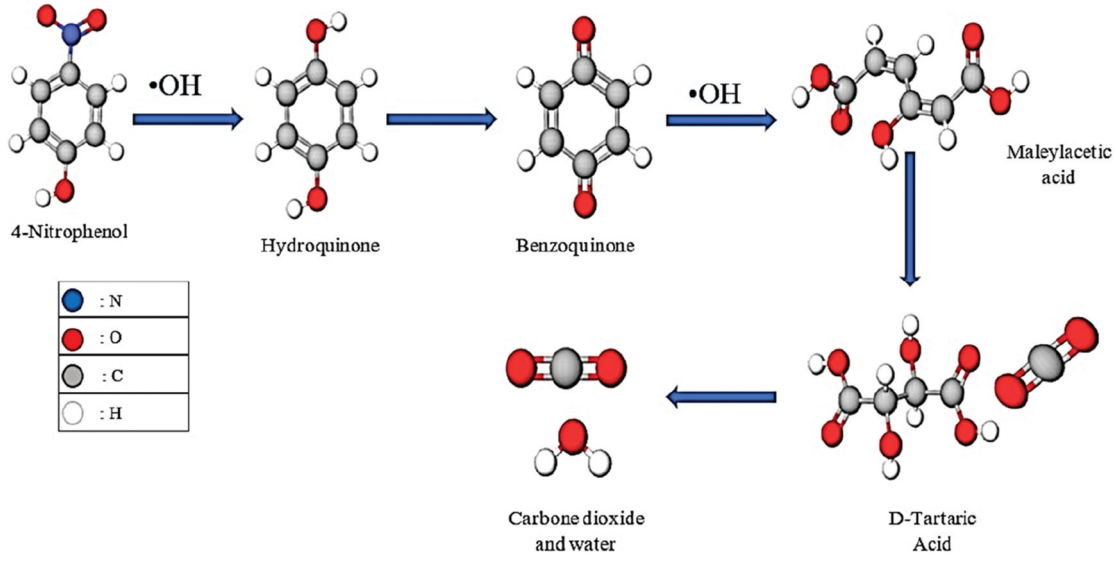


Figure 18. Proposed reaction mechanism for 4-nitrophenol degradation by OH• generated by catalytic ozonation in aqueous solution.

In order to represent our phenomena, it is required to draw the line of $\ln([4NP]_0/[4NP])$ as a function of time (Figure 16) and (Figure 17). We can use this information to determine the reaction's rate constant.

The ozonation rate constant of 4NP with CuAl-$CO_3$ (K' = 0,984 $min^{-1}$). was found to be greater than that of $CuAl_{500}$ (K' = 0.624 $min^{-1}$), indicating the efficiency of the carbonated catalyst.

Figure 18 depicts the simplified reaction mechanism proposed by P.V.R.K. Ramacharyulu and its collaborators (Ramacharyulu et al. 2018) for the degradation of 4Nitrophenol in the presence of hydroxyl radicals generated by catalytic ozonation in aqueous solution, where the first attack serves to eliminate the nitro group, then a series of reactions resulting from the reaction intermediates take place to obtain only water and carbon

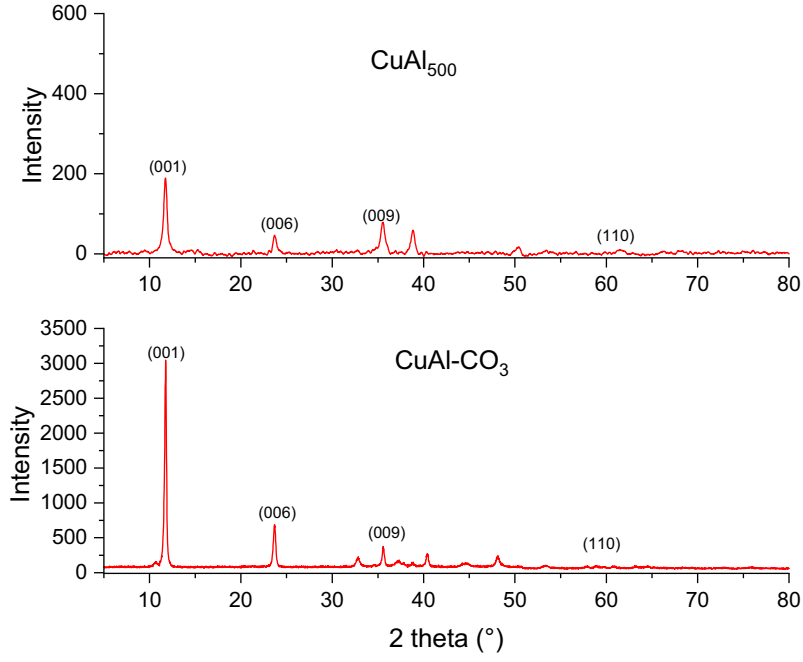


**Figure 19.** XRD diffractograms of catalysts recovered after catalytic ozonation reaction of 4NP.

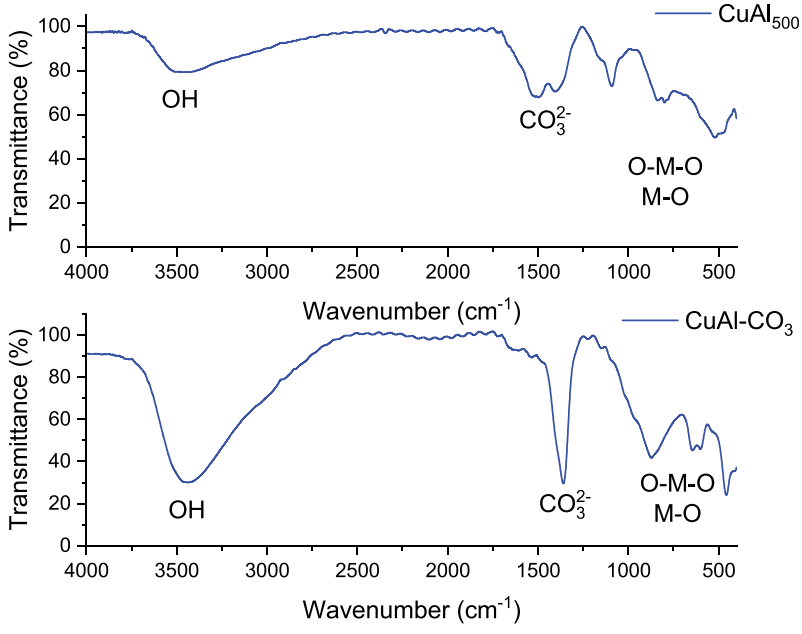


**Figure 20.** FTIR spectrum of catalysts recovered after catalytic ozonation reaction of 4NP.

dioxide at the end of the reaction, followed by total mineralization of the starting product.

The CuAl-$CO_3$ and $CuAl_{500}$ catalysts are examined by FTIR and XRD after recovery and washing with distilled water in order to assess their crystalline morphologies and primary uses. Figure 19's XRD results show that the crystalline structure of CuAl-$CO_3$ has not changed, in contrast to $CuAl_{500}$, where we see a slight crystallization of the hydrotalcite type. This crystallization is caused by the memory effect, which is a property of hydrotalcite products when they reassemble in the presence of ions.

The FTIR shown in Figure 20 can be used to confirm the intercalation of new ions since it clearly depicts the emergence of the OH and carbonate characteristic bands in the calcined catalyst $CuAl_{500}$.

## Conclusion

The aim of this study was to analyze the effectiveness of a copper-based hydrotalcite catalyst and its oxide derivative for removing 4NP pollutants from municipal wastewater. The CuAl-$CO_3$ material was produced by co-precipitation at a constant pH, and the derived oxide was obtained by calcination of the CuAl-$CO_3$ carbon phase at a specific temperature determined by TGA analysis. XRD of the carbonate phase shows diffraction similar to hydrotalcite, copper oxide was detected in the calcined phase using the COD 2019 database. FTIR analysis confirmed the efficiency of carbonate phase synthesis by identifying the vibrational modes of the chemical processes. This also proves that the calcination process loses water and carbonate ions, forming an oxide phase. EDS analysis confirmed the disappearance of carbon due to calcination and deoxygenation. SEM-EDS confirms CuAl-$CO_3$ is a hexagonal crystal, and $CuAl_{500}$ is a perfectly shaped sand rose. The pHpzc values of CuAl-$CO_3$ and $CuAl_{500}$ are 6.1 and 7.4, respectively. CuAl-$CO_3$ LDH was used to optimize the experimental parameters (catalyst mass, pH and temperature). The optimal pH of the reaction is 11, and 0.3 g. $L^{-1}$ was the mass effectively eliminated 78.6% of 100 mg. $L^{-1}$ of 4NP. Ozonation is most effective at 10 or 55 °C due to the inhibition of ozone outgassing at low temperatures and kinetic effects at high temperatures. A kinetic study was performed to compare the efficiency of the two catalysts. It was found that the ozonation rate constant of 4NP with CuAl-$CO_3$ was higher than that of $CuAl_{500}$, confirming the effectiveness of carbonated catalyst. COD removal in 4 h was studied to compare the efficiency of two types of catalysts. The calcined phase is reorganized thanks to the memory effect of the hydrotalcite material, shown through post-use analysis, recovery and XRD. FTIR also detected OH and carbonate bands in the calcination phase, indicating the different ways in which calcination is needed to regenerate the catalyst. The results show the effectiveness of lamellar double hydroxide in catalyzing the ozonation of 4NP. However, further research is needed to understand the selectivity of the catalyst when using real wastewater. To determine reusability, the material must be reused after regeneration. Finally, the combination with UV light is recommended to study the synergistic effect on the oxidation of organic pollutants in urban wastewater.

## Acknowledgments

Abderrahmane HIRI expresses gratitude to the University of Adrar for permitting the completion of this study in its facilities. He also thanks the Technical Platform for Physicochemical Analyzes (PTAPC-Laghouat-CRAPC and PTAPC-Ouargla-CRAPC) in Algeria, the Directorate General for Scientific Research and Technological Development (DGRSDT), the Catalysis and Materials for the Environment and Processes Research Laboratory LRCMEP (LR19ES08) in university of Gabès Tunisia, and all of the staff members working at the four laboratories.

## Disclosure statement

No potential conflict of interest was reported by the author(s).

## ORCID

Abderrahmane Hiri http://orcid.org/0000-0002-1438-8961
Ghania Radji http://orcid.org/0000-0002-8000-7653
Rania Amiri http://orcid.org/0009-0001-3993-6899
Achour Dakhouche http://orcid.org/0000-0002-8598-6678
Kamel Noufel http://orcid.org/0000-0001-8253-7204

## References

Arasteh, R., M. Masoumi, A. M. Rashidi, L. Moradi, V. Samimi, and S. T. Mostafavi. 2010. "Adsorption of 2-Nitrophenol by Multi-Wall Carbon Nanotubes from Aqueous Solutions." *Applied Surface Science* 256 (14): 4447–55. https://doi.org/10.1016/j.apsusc.2010.01.057.

Beltran, F. J. 2003. *Ozone Reaction Kinetics for Water and Wastewater Systems*. 1st ed. Florida: Lewis Publishers. https://doi.org/10.1201/9780203509173.

Benito, P., I. Guinea, F. M. Labajos, and V. Rives. 2008. "Microwave-Assisted Reconstruction of Ni,al Hydrotalcite-Like Compounds." *Journal of Solid State Chemistry* 181 (5): 987–96. https://doi.org/10.1016/j.jssc.2008.02.003.

Cavani, F., F. Trifirò, and A. Vaccari. 1991. "Hydrotalcite-Type Anionic Clays: Preparation, Properties and Applications." *Catalysis Today* 11 (2): 173–301. https://doi.org/10.1016/0920-5861(91)80068-K.

Chen, J., X. Sun, L. Lin, X. Dong, and Y. He. 2017. "Adsorption Removal of O-Nitrophenol and P-Nitrophenol from Wastewater by Metal–Organic Framework Cr-BDC." *Chinese Journal of Chemical Engineering* 25 (6): 775–81. https://doi.org/10.1016/j.cjche.2016.10.014.

Choi, Y., K. Tan Lee, and K. Bong Lee. 2023. "Novel Layered Double Hydroxide-Based Passive NOx Adsorber: Synergistic Effects of Co and Mn on Low-Temperature NOx Storage and Regeneration." *Separation and Purification Technology* 324 (x): 124391. https://doi.org/10.1016/j.seppur.2023.124391.

Degrémont-Suez, Rueil-Malmaison, C. diff. Lavoisier, edited by, 4. OXYDATION ET DÉSINFECTION PAR L'OZONE," in *Mémento technique de l'eau - Tome 1*, Degrémont, 2005, pp. 880–91.

Deng, F., Zhang Q., Yang L., Luo X., Wang A., Luo S., and Dionysiou D. D. 2018. "Visible-Light-Responsive Graphene-Functionalized Bi-Bridge Z-Scheme Black BiOcl/Bi2O3 Heterojunction with Oxygen Vacancy and Multiple Charge Transfer Channels for Efficient Photocatalytic Degradation of 2-Nitrophenol and Industrial Wastewater Treatment." *Applied Catalysis B: Environmental* 238:61–69. https://doi.org/10.1016/j.apcatb.2018.05.004.

Dubey, A., V. Rives, and S. Kannan. 2002. "Catalytic Hydroxylation of Phenol Over Ternary Hydrotalcites Containing Cu, Ni and Al." *Journal of Molecular Catalysis A, Chemical* 181 (1–2): 151–60. https://doi.org/10.1016/S1381-1169(01)00360-0.

Gottschalk, C., J. A. Libra, and A. Saupe. 2010. *Ozonation of Water and Waste Water: A Practical Guide to Understanding Ozone and Its Applications*. 2nd ed. WeinheimI: John Wiley & Sons.

Guzman-Perez, C. A., J. Soltan, and J. Robertson. 2011. "Kinetics of Catalytic Ozonation of Atrazine in the Presence of Activated Carbon." *Separation and Purification Technology* 79 (1): 8–14. https://doi.org/10.1016/j.seppur.2011.02.035.

Hamidouche, S., O. Bouras, F. Zermane, B. Cheknane, M. Houari, J. Debord, M. Harel, et al. 2015. "Simultaneous Sorption of 4-Nitrophenol and 2-Nitrophenol on a Hybrid Geocomposite Based on Surfactant-Modified Pillared-Clay and Activated Carbon." *Chemical Engineering Journal* 279:964–72. https://doi.org/10.1016/j.cej.2015.05.012.

Huang, T., G. Zhang, S. Chong, Y. Liu, N. Zhang, S. Fang, J. Zhu, et al. 2017. "Effects and Mechanism of Diclofenac Degradation in Aqueous Solution by US/Zn0." *Ultrasonics Sonochemistry* 37:676–85. https://doi.org/10.1016/j.ultsonch.2017.02.032.

Kordić, B., B. Jović, J. Tričković, and M. Kovačević. 2018. "Adsorption of Selected Nitrophenols on Activated Carbon in the Presence of Nicotinamide." *Journal of Molecular Liquids* 259:7–15. https://doi.org/10.1016/j.molliq.2018.02.109.

Kupeta, A. J. K., E. B. Naidoo, and A. E. Ofomaja. 2018. "Kinetics and Equilibrium Study of 2-Nitrophenol Adsorption Onto Polyurethane Cross-Linked Pine Cone Biomass." *Journal of Cleaner Production* 179:191–209. https://doi.org/10.1016/j.jclepro.2018.01.034.

Mahmoud, M. E., and G. M. Nabil. 2017. "Nano Zirconium Silicate Coated Manganese Dioxide Nanoparticles: Microwave-Assisted Synthesis, Process Optimization, Adsorption Isotherm, Kinetic Study and Thermodynamic Parameters for Removal of 4-Nitrophenol." *Journal of Molecular Liquids* 240:280–90. https://doi.org/10.1016/j.molliq.2017.05.075.

Mak Yu, T., A. Caroline Reis Meira, J. Cristina Kreutz, L. Effting, R. Mello Giona, R. Gervasoni, A. Amado de Moura, F. Maestá Bezerra, and A. Bail. July 2019. "Exploring the surface reactivity of the magnetic layered double hydroxide lithium-aluminum: An alternative material for sorption and catalytic purposes." *Applied Surface Science* 467–468:1195–203. 2018. https://doi.org/10.1016/j.apsusc.2018.10.221.

Mishra, G., B. Dash, and S. Pandey. 2018. "Layered Double Hydroxides: A Brief Review from Fundamentals to Application as Evolving Biomaterials." *Applied Clay Science* 153 (October): 172–86. 2017. https://doi.org/10.1016/j.clay.2017.12.021.

Orfei, E., A. Fasolini, S. Abate, N. Dimitratos, and F. Basile. 2023. "Layered-Double Hydroxides and Derived Oxide as CRM-Free Highly Active Catalysts for the Reduction of 4-Nitrophenol." *Catalysis Today* 419 (November): 114153. 2022. https://doi.org/10.1016/j.cattod.2023.114153.

Pavlovic, I., M. A. Ulibarri, and M. C. Hermosı. 2002. *Hydrotalcites as Sorbent for 2, 4, 6-Trinitrophenol : Influence of the Layer Composition and Interlayer Anion* 1027–34. https://doi.org/10.1039/b107979b.

Prikhod'ko, R. V., M. V. Sychev, I. M. Astrelin, K. Erdmann, A. Mangel, and R. A. Van Santen. 2001. "Synthesis and Structural Transformations of Hydrotalcite-Like Materials Mg-Al and Zn-Al." *Russian Journal of Applied Chemistry* 74 (10): 1621–26. https://doi.org/10.1023/A:1014832530184.

Radji, G., N. Bettahar, A. Bahmani, I. Boukhetache, and S. Contreras. 2022. "Heterogeneous Fenton-Like Degradation of Organic Pollutants in Petroleum Refinery Wastewater by Copper-Type Layered Double Hydroxides." *Journal of Water Process Engineering* 50 (July): 103305. https://doi.org/10.1016/j.jwpe.2022.103305.

Rajamathi, M., and P. V. Kamath. 2003. "Anionic Clay-Like Behaviour of α-Nickel Hydroxide: Chromate Sorption Studies." *Materials Letters* 57 (16–17): 2390–94. https://doi.org/10.1016/S0167-577X(02)01240-5.

Ramacharyulu, P. V. R. K., S. J. Abbas, S. R. Sahoo, and S. C. Ke. 2018. "Mechanistic Insights into 4-Nitrophenol Degradation and Benzyl Alcohol Oxidation Pathways Over MgO/g-C3N4 Model Catalyst Systems." *Catalysis Science & Technology* 8 (11): 2825–34. https://doi.org/10.1039/c8cy00431e.

Shao, L., and J. Huang. 2017. "Controllable Synthesis of N-Vinylimidazole-Modified Hyper-Cross-Linked Resins and Their Efficient Adsorption of P-Nitrophenol and O-Nitrophenol." *Journal of Colloid and Interface Science* 507:42–50. https://doi.org/10.1016/j.jcis.2017.07.112.

Shokri, Aref. 2016. "Degradation of 4-Nitrophenol from Industerial Wastewater by Nano Catalytic Ozonation Young Researchers and Elite Club, Arak Branch, Islamic

Azad University, Arak, Iran Re." *International Journal of Nano Dimension* 7 (2): 160–67. https://doi.org/10.7508/ijnd.2016.02.008.

Shokri, A., K. Mahanpoor, and D. Soodbar. 2016. "Degradation of Ortho-Toluidine in Petrochemical Wastewater by Ozonation, UV/O3, O3/H2O2 and UV/O3/H2O2 Processes." *Desalination & Water Treatment* 57 (35): 16473–82. https://doi.org/10.1080/19443994.2015.1085454.

Sumegová, L., J. Derco, and M. Melicher. 2013. "Influence of Reaction Conditions on the Ozonation Process." *Acta Chimica Slovaca* 6 (2): 168–72. https://doi.org/10.2478/acs-2013-0026.

Taishi, Y., K. Tsukada, S. Terasaka, M. Kamitakahara, and H. Matsubara. 2015. "Morphological Control of Layered Double Hydroxide Through a Biomimetic Approach Using Carboxylic and Sulfonic Acids." *Journal of Asian Ceramic Societies* 3 (3): 230–33. https://doi.org/10.1016/j.jascer.2015.05.004.

Van, K., D. L. Steven, and A. B. William. 1980. "Ambient Water Quality Criteria for Nitrophenols." *Catologuing Public Data John, Autian* 2 (October): 160.

Xu, Z. P., and H. C. Zeng. 1998. "Thermal Evolution of Cobalt Hydroxides: A Comparative Study of Their Various Structural Phases." *Journal of Materials Chemistry* 8 (11): 2499–506. https://doi.org/10.1039/a804767g.

Zaggout, F. R., and N. Abu Ghalwa. 2008. "Removal of O-Nitrophenol from Water by Electrochemical Degradation Using a Lead Oxide/Titanium Modified Electrode." *Journal of Environmental Management* 86 (1): 291–96. https://doi.org/10.1016/j.jenvman.2006.12.033.

Zhang, Y., M. Mei, X. Huang, and D. Yuan. 2015. "Extraction of Trace Nitrophenols in Environmental Water Samples Using Boronate Affinity Sorbent." *Analytica chimica acta* 899:75–84. https://doi.org/10.1016/j.aca.2015.10.004.

Zhang, H., K. Zou, H. Sun, and X. Duan. 2005. "A Magnetic Organic-Inorganic Composite: Synthesis and Characterization of Magnetic 5-Aminosalicylic Acid Intercalated Layered Double Hydroxides." *Journal of Solid State Chemistry* 178 (11): 3485–93. https://doi.org/10.1016/j.jssc.2005.09.008.